Ceramics-Silikáty 63 (1), 1-10 (2019)
www.ceramics-silikaty.cz doi: 10.13168/cs.2018.0040

MICROSTRUCTURE, MECHANICAL PROPERTIES AND FRICTION/WEAR BEHAVIOR OF HOT-PRESSED Si_3N_4/BN CERAMIC COMPOSITES

#WEI CHEN*, ZHAOXUN WANG*, YIMIN GAO**, HUAQIANG LI***, NAIRU HE*

*College of Mechanical and Electrical Engineering, Shaanxi University of Science & Technology, Xi'an 710021, P.R. China
**State Key Laboratory for Mechanical Behavior of Materials, Xi'an Jiaotong University, Xi'an 710049, P.R. China
***Guangdong JOOYN New Material Technology Co.,Ltd., Xi'an 710065, P.R. China

#E-mail: chenweijd@sust.edu.cn

Submitted July 12, 2018; accepted September 11, 2018

Keywords: Friction Mechanisms, Ceramic Composite, Unlubricated Wear, Silicon nitride (Si_3N_4), Boron Nitride (BN)

Nano-scale and micro-scale hexagonal boron nitride (hBN) powders, respectively, were added to silicon nitride (Si_3N_4) matrix powder, and Si_3N_4/BN ceramic composites with different content of solid-lubrication hBN were produced by hot pressing. The combined effect of starting powder and hBN content on the microstructure, mechanical properties and tribological properties of Si_3N_4/BN ceramic composites has been studied. The results showed that the nano-sized starting powder was beneficial to the densification of Si_3N_4/BN ceramic composites, and resulted in a Si3N4/BN nano/nano ceramic composite with slightly higher density and improved mechanical properties compared to the corresponding micro/nano ceramic composite. The physical and mechanical properties of Si_3N_4-based ceramic composites were found to be affected by addition of BN. Increasing BN content led to a decrease of bulk density, hardness, bending strength and fracture toughness. On the other hand, the starting powder has no significant influence on the tribological properties of Si_3N_4/BN ceramic composites. The friction properties and wear resistance continuously improved with increasing BN content up to 20 vol. %, due to the formation of tribochemical film composed of H_3BO_3, SiO_2 and metal oxides.

INTRODUCTION

Ceramic composites are ceramic materials that have been gradually developed since the 1980s. They can have excellent properties, such as high temperature resistance, wear resistance, temperature creep resistance, chemical corrosion resistance, high strength, high hardness, as well as tailorable thermal conductivity, thermal expansion coefficient, and dielectricity [1-5]. Hence, ceramic composites can be widely used in cases where organic materials and metal materials cannot satisfy the performance requirements of the operating conditions, which is the reason why ceramics and ceramic composites have become ideal high-temperature structural materials. Moreover, nanoceramics are new high-performance ceramic materials developed in recent years. Compared with ordinary ceramic materials, nanoceramics have obvious advantages with regard to their mechanical properties, surface roughness, wear resistance, and high-temperature performance [6].

Silicon nitride (Si_3N_4) is widely used in engineering, because of its high strength, high hardness, wear resistance, corrosion resistance, high temperature resistance, low density, self-lubrication, and excellent electrical insulation. However, due to the inherent mechanical properties of Si_3N_4 ceramics (such as brittleness), their poor machinability and dry friction property their engineering applications are somewhat limited [7]. However, recent research has shown that the addition of proper second phases (such as graphite, carbon nanotubes, or hexagonal boron nitride / hBN)) into Si_3N_4 matrix can significantly improve the tribological properties and machinability.

Kvetková et al. [8] prepared Si_3N_4-graphene platelet (GPL) composites via hot isostatic pressing (HIP). The results showed that The GPLs were located at the boundaries of Si_3N_4, and hindered the grain growth and change the shape of the grains. In this case, the addition of GPLs into Si_3N_4 matrix improved the fracture toughness, but lowered the hardness of Si_3N_4 ceramics. Meanwhile, Hvizdoš et al. [6] prepared Si_3N_4-graphene platelet (GPL) composites via HIP and studied their tribological properties. The results showed that the addition of carbon phases did not significantly lower the coefficient of friction. Graphene platelets seemed to be integrated into the matrix very strongly and they do not participate in lubricating processes, resulting in higher friction and wear. It is well known, however, that hexagonal boron nitride (hBN) processes a number of interesting properties such as self-lubrication, low friction coefficient and low hardness. Si_3N_4 ceramics containing hBN (micro-sized or nano-sized) were prepared via the HIP method by Kovalčíková [9]. The results showed that the increase of hBN content resulted in a sharp decrease

of hardness, elastic modulus and bending strength of Si_3N_4/BN composites. The authors also found that the friction coefficient was not influenced by BN addition to Si_3N_4/BN composites. However, our previous research showed that Si_3N_4/BN composites (micro-sized) showed better tribological properties [10-14]. Especially, a lower friction coefficient (0.03) and wear rates of order 10^{-6} were obtained for a sliding pair of Si_3N_4/BN composite and stainless steel, which is attributed to the formation of a self-lubricating film composed of SiO_2, H_3BO_3 and Fe_2O_3. Interestingly, Kusunose [15] found that the drilled surface of Si_3N_4/BN nanocomposites showed minor damage compared with microcomposites. The excellent machinability was attributed to quasi-plasticity of the composites. These findings suggest a significant potential of Si_3N_4/BN nanocomposites, but further studies are needed in order to fully understand the effect of composition on their microstructure development, mechanical and tribological properties.

The aim of the present contribution is to investigate the influence of hBN content on the microstructure development, mechanical and tribological performances of Si_3N_4/BN nanocomposites.

EXPERIMENTAL

Materials

In this work, two types of materials were prepared. The first group were samples in which micro-sized Si_3N_4 particles were mixed with nano-sized hBN particles (Si_3N_4/hBN micro/nano-composites). The second group were samples in which nano-sized Si_3N_4 particles were mixed with nano-sized hBN particles (Si_3N_4/hBN nano/nano-composites). The starting powders were commercial micro- or nano-sized Si_3N_4 particles (purity > 99.9 %, α phase content > 93 %, average particle size of 1.5 μm/ /40 - 50 nm, HeFei Aijia New Material Co., Ltd.) with 4 % Y_2O_3 (purity > 99 %, average particle size of 0.37 μm) and 6 % Al_2O_3 (purity > 99 %, average particle size of 1.17 μm) as sintering additives. Nano-sized hBN particles (purity > 99 %, average particle size of 60 - 80 nm, HeFei Aijia New Material Co., Ltd.) were used as a solid lubricant phase. The volume fraction of solid lubricant additions was 0 %, 5 %, 10 %, 20 %, or 30 %, respectively. Figure 1 shows the X-ray diffraction (XRD) results of the silicon nitride powder and the hBN powder.

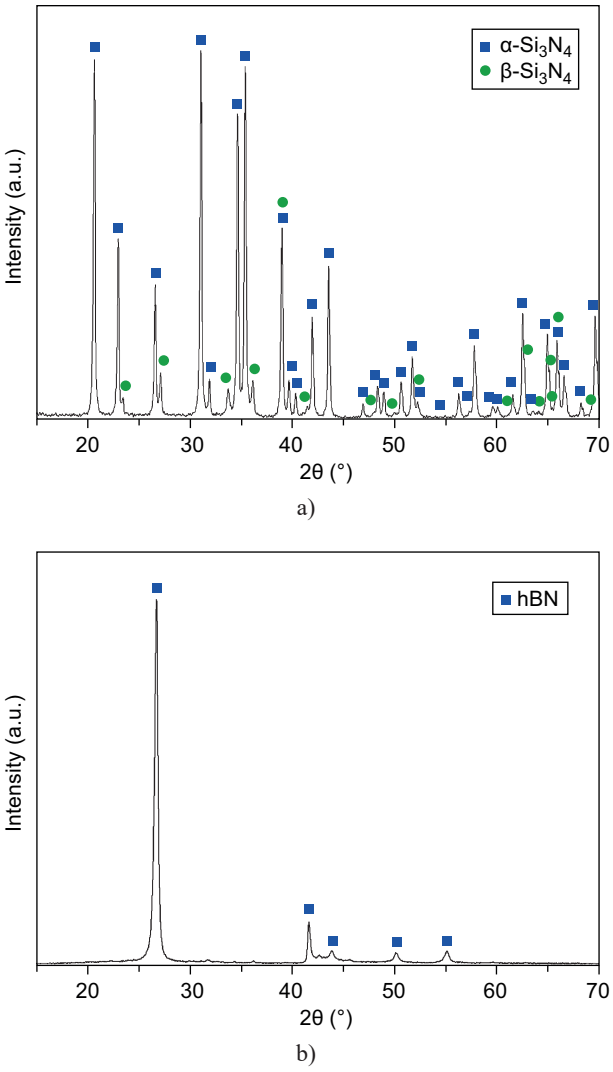

Figure 1. X-ray diffraction results of starting powders: a) Si_3N_4 and b) hBN.

Table 1. Composition of the starting powders and powder mixture.

Samples	Starting powders (vol. %)			Additive (vol. %)	Preparation of powder mixtrure
	Si_3N_4	Al_2O_3	Y_2O_3	hBN	
SN-m0	90	6	4	0	micro-sized Si_3N_4 powders
SN-m5	90	6	4	5	micro-sized Si_3N_4 + nano-sized hBN powders
SN-m10	90	6	4	10	micro-sized Si_3N_4 + nano-sized hBN powders
SN-m20	90	6	4	20	micro-sized Si_3N_4 + nano-sized hBN powders
SN-m30	90	6	4	30	micro-sized Si_3N_4 + nano-sized hBN powders
SN-n0	90	6	4	0	nano-sized Si_3N_4 powders
SN-n5	90	6	4	5	nano-sized Si_3N_4 + nano-sized hBN powders
SN-n10	90	6	4	10	nano-sized Si_3N_4 + nano-sized hBN powders
SN-n20	90	6	4	20	nano-sized Si_3N_4 + nano-sized hBN powders
SN-n30	90	6	4	30	nano-sized Si_3N_4 + nano-sized hBN powders

The combined powders were mixed and ball-milled in alcohol for 24 h. After the slurry was dried, the powders were hot-pressed sintering (HP). In HP, the powders were hot-pressed in flowing N_2 at 1800°C for 30 min in an hBN-coated graphite die to produce a disc. A pressure of 30 MPa was employed to fabricate the Si_3N_4/BN composites. The chemical composition and way of sintering is briefly summarized in Table 1.

Test procedure

The densities of the sintered specimens were measured according to Archimedes' principle. Phase compositions were determined by X-ray diffraction with Cu K_α radiation. Sintered specimens were grinded, polished to a 1 μm finish by routine ceramographic procedures and chemically etched in molten NaOH at 400 °C for 2 min. The microstructures were then studied by using an SEM.

Mechanical properties were investigated using indentation methods. Hardness was determined by Vickers indentation under a load of 10 N with a dwell time of 15 s. In order to determine the indentation toughness, at least 5 Vickers indentations per specimen were made on the basis of Vickers hardness measurements. The indentation toughness was calculated from the lengths of radial cracks and indents diagonals using a formula given as follows [16]:

$$K_{IC} = 0.203 \times (c/a)^{-3/2} \cdot a \cdot HV \qquad (1)$$

where, a is the half length of indentation diagonal, c is the radial half-crack length and HV is Vickers hardness of materials.

The three-point bending strength values for samples were determined by bending tests using specimens with dimensions 3 × 4 × 30 mm. The specimens were tested in a three-point bending fixture (span of 20 mm) with a crosshead speed of 0.5 mm·min^{-1} at ambient temperature and atmosphere.

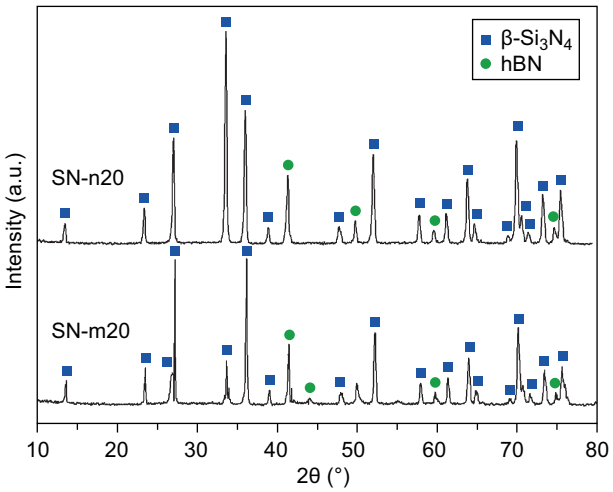

Figure 2. XRD patterns of the Si_3N_4/BN composites: SN-n20 and SN-m20.

Wear testing was carried out at room temperature on a pin-on-disc tribometer. The ceramic pin (in the size of 5 × 5 × 5 mm) surfaces were carefully prepared by polishing down to surface roughness below 0.05 μm where possible. Wear behavior of the prepared materials was studied in dry sliding, where the tribological counterpart was a highly polished GCr15 disc with 44 mm in diameter and 6 mm in thickness. A normal load of 10 N and a sliding speed of 0.86 m·s^{-1} (namely, 500 r·min^{-1}) were applied. Total sliding time was 10 min (600 s). The friction coefficients were continually recorded by the tester and further processed by its data processing software. The volume wear rate V_m is given by $V_m = \Delta m/(PS\rho)$, where V_m (mm^3·Nm^{-1}) is the volume wear rate, Δm (g) the mass loss weighed by microbalance with accuracy 0.1 mg, P (N) the normal load, S (m) the sliding distance, and ρ (g·cm^{-3}) the bulk density of the specimen. The wear surfaces of the investigated materials were studied using SEM to identify the wear mechanisms.

RESULTS AND DISCUSSION

Phase composition

Figure 2 shows the XRD patterns of the Si_3N_4/20 % BN micro/nano-composites and Si_3N_4/20 % BN nano/nano-composites. The figure shows that complete transformation from α- to β-Si_3N_4 was achieved in all specimens and that diffraction peaks of β-Si_3N_4 phase and hBN phase exist in the XRD patterns of both the Si_3N_4/BN micro/nano-composites and the Si_3N_4/BN nano/nano-composites. The highest diffraction peak of the hBN phase was at 2θ = 41.34°, and other smaller diffraction peaks also correspond to the hBN phase.

Microstructure

Figure 3 illustrates the microstructures of the monolithic Si_3N_4 ceramics prepared with micro-sized and nano-sized powders, respectively. The microstructure of the sintered SN-n0 specimen (Figure 3a) consisted mainly of elongated β-Si_3N_4 grains, granular grains and inter-granular phase. Compared with SN-n0, the SN-m0 specimen (Figure 3b) represents an apparently more porous surface, consisting of larger elongated grains, granular grains and more voids (possibly due to grain pull-out during grinding). The nano-sized starting powder seems to be beneficial to the strengthening and densification of monolithic Si_3N_4 ceramics, but the differences concerning grain size are surprisingly small, i.e. the ceramic SN-n0, made from the nano-scale powder, is not much finer than the ceramic SN-m0, made from the micro-scale powder.

Figure 4 shows the microstructures of the Si_3N_4/20 % BN nano/nano-composite and micro/nano-composite. The microstructures of Si_3N_4/20 % BN composites

consists of elongated β-Si_3N_4 grains, equiaxed β-Si_3N_4 grains, hBN particles and intergranular phase. It can be seen from Figure 4a, that some hBN agglomerates were found in the SN-n20 nano/nano-composites. However, the influence on the diameter and aspect ratio of Si_3N_4 grains is not very significant when the hBN content is increased to 20 %. From Figure 4b it follows, that agglomerates are found also in SN-m20. The densification of composites is inhibited by agglomeration of hBN between the Si_3N_4 boundaries. Thus, the porosity of specimens with hBN addition was remarkably larger than that of monolithic specimens.

Physical and mechanical properties of ceramic composites

The monolithic Si_3N_4 nano-ceramic had the highest bulk density with a value of 3.20 g·cm^{-3}, as shown in Figure 5. The density of Si_3N_4/BN nano/nano-composites and micro/nano-composites were in intervals from 2.81 to 3.20 g·cm^{-3} and 2.94 to 3.18 g·cm^{-3}, respectively. The reduction in bulk density with the increase of hBN content could be attributed to the low density of hBN (ρ_{hBN} = 2.27 g·cm^{-3}) and the low chemical reactivity of hBN in Si_3N_4/BN composites [7]. In addition, and the bulk density of Si_3N_4/BN nano/nano-composites

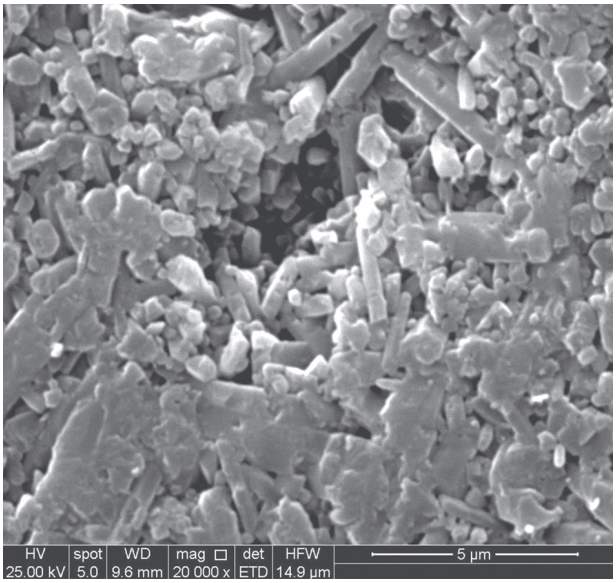

a) SN-n0

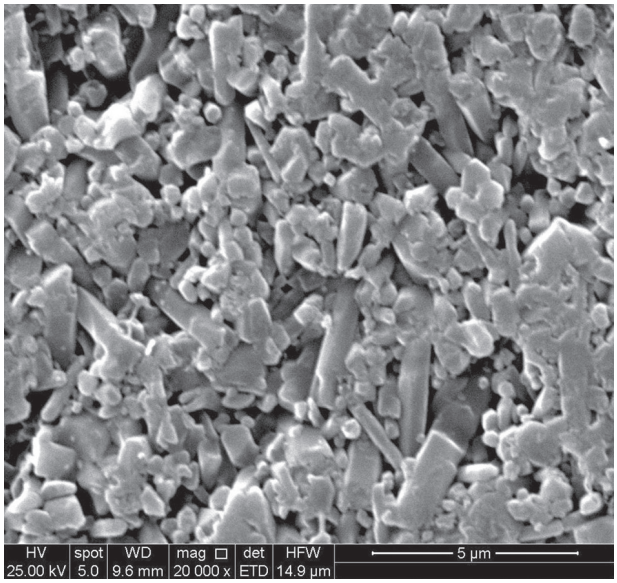

b) SN-m0

Figure 3. SEM images of monolithic Si_3N_4 ceramic: a) SN-n0; b) SN-m0.

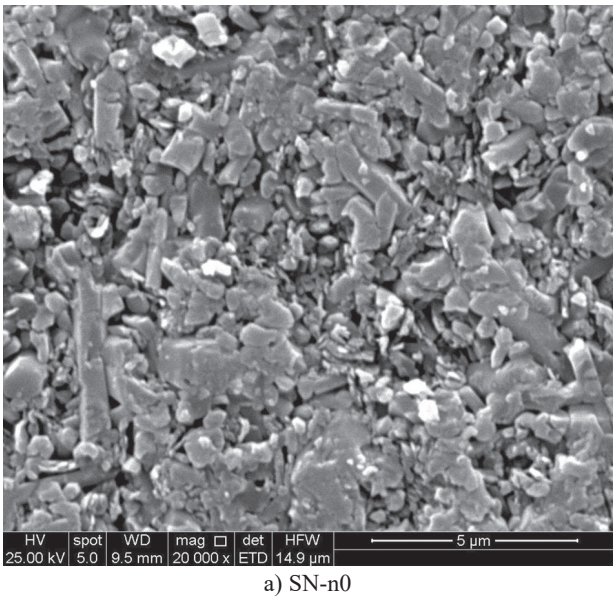

a) SN-n0

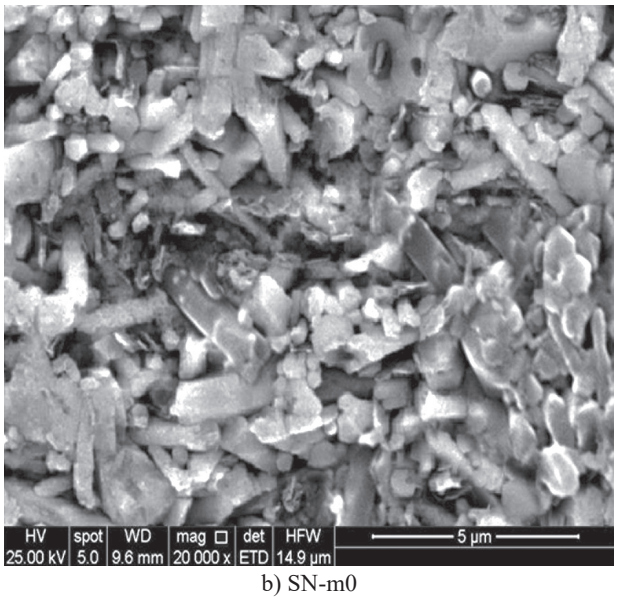

b) SN-m0

Figure 4. SEM images of Si_3N_4/BN composites: a) SN-n20; b) SN-m20.

is slightly higher than that of micro/nano-composites, probably due to the higher sintering activity of the nano-size Si_3N_4, see Figure 3.

The influence of hBN content on Vicker's hardness, bending strength and fracture toughness of Si_3N_4/BN composites was investigated. Figure 6 shows the relation of composite hardness versus the hBN content. It is obviously that the Vicker's hardness of Si_3N_4/BN composites decreased with increasing hBN volume fraction. Easy cleavage of basal plane of hBN platelets causes both hardness and bending strength (as shown in Fig. 7) to decrease with hBN addition [17].

Moreover, the incorporation of hBN seems to support crack propagation and thus reduce the fracture toughness of the composite. Figure 8 shows the fracture toughness values of monolithic Si_3N_4 and composites. The fracture toughness of Si_3N_4/BN composites decreased with the increase of hBN content, and the nano/nano-composites tended to perform slightly better than the micro/nano-composites. Some investigators have shown that adding a small quantity of hBN to Si_3N_4 can increase the fracture toughness of Si_3N_4 ceramic matrix [18-19], which could be attributed to grain refinement. However, the addition up to 30 wt. % BN had only a very small influence on the diameter of Si_3N_4 grains in our study, as shown in Figures 9a and 9b. Moreover, Figure 9c shows the micrographs of micro-sized Si_3N_4 ceramics, and it indicates that the grains of micro-sized Si_3N_4 ceramics are significantly larger than those of the nano-sized Si_3N_4 ceramics (as shown in Figure 9a). So, it can be concluded that the starting powder has a slight influence on the grain size of composites, resulting in the difference between micro/nano-composites and nano/nano-composites. In addition, different toughening mechanisms, such as pull-out of elongated β-Si_3N_4 grains (the region indicated by white arrows in Figure 10), grain cracking (intragranular fracture) and pull-out of hBN platelets, as shown in the high magnification micrographs of composite fracture surfaces (as shown in Figure 10). Also hBN agglomerates were found in the composites in the figure (the region indicated by white circle in Figure 10). From the results above, the addition of hBN content resulted in reduction

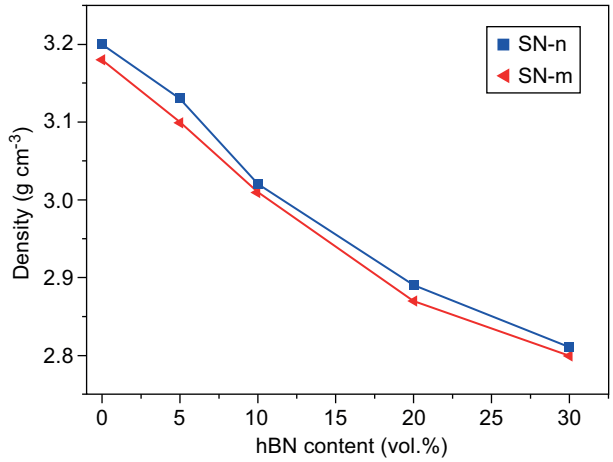

Figure 5. Effect of hBN content on the density of Si_3N_4/BN composites.

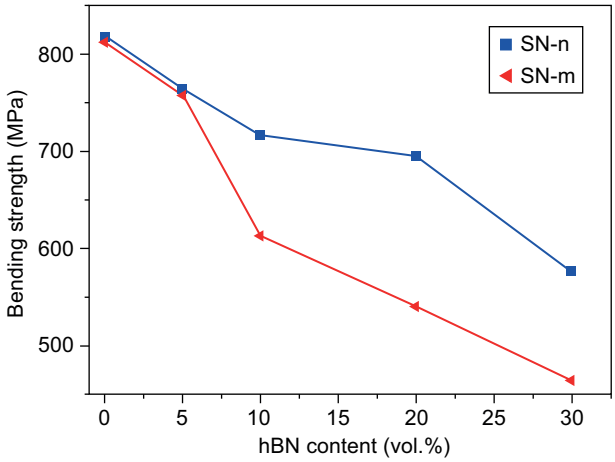

Figure 7. Effects of the hBN content on the bending strength of Si_3N_4/BN composites.

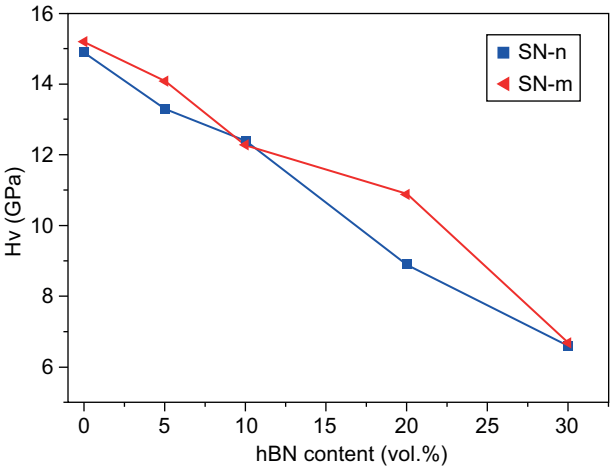

Figure 6. Effects of the hBN content on the hardness of Si_3N_4/BN composites.

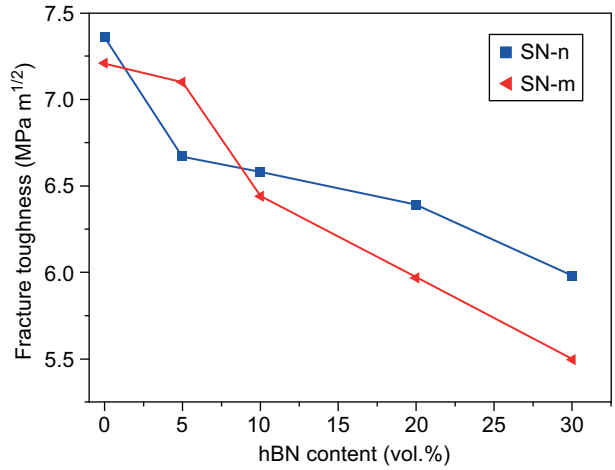

Figure 8. Effects of the hBN content on the fracture toughness of Si_3N_4/BN composites.

of mechanical properties of Si_3N_4/BN composites, and the mechanical properties are slightly affected by the starting powder.

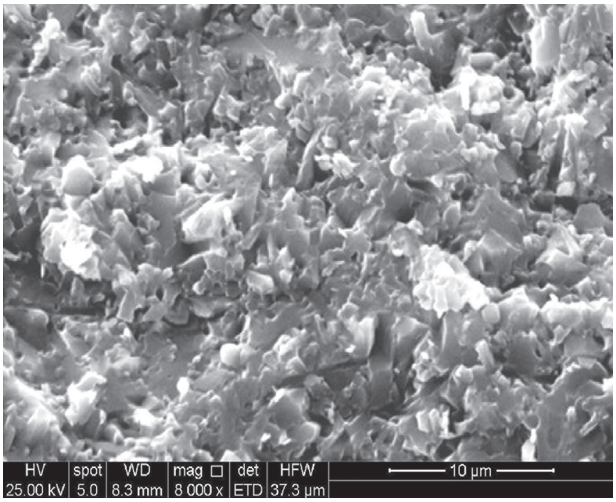

a) SN-n0

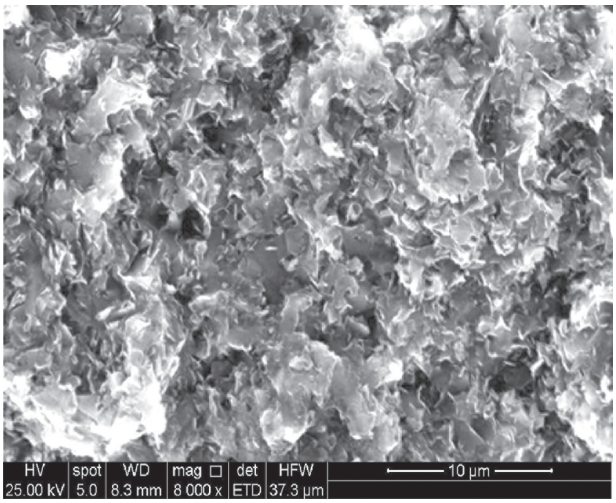

b) SN-n30

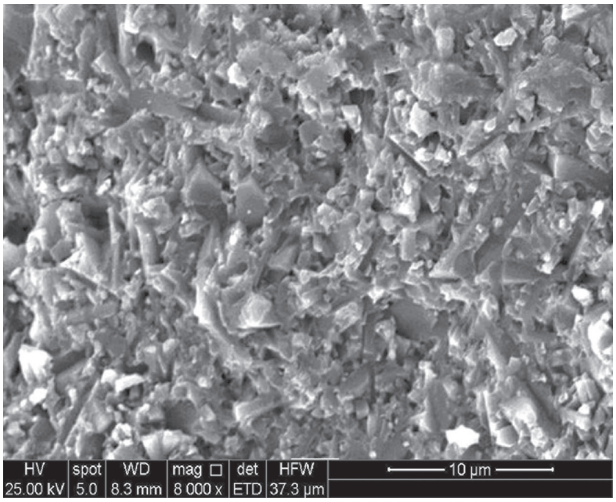

c) SN-m0

Figure 9. SEM micrographs of fracture surfaces of a) SN-n0; b) SN-n30 and c) SN-m0.

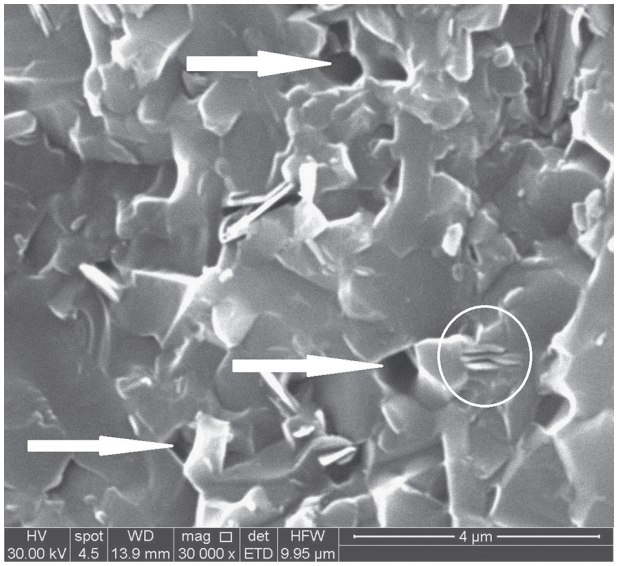

Figure 10. High magnification SEM image of fracture surface of SN-n5 composite.

Tribological properties

Figure 11 shows the average values of the friction coefficients for all composites in contact with GCr15 disc. The friction coefficient of monolithic Si_3N_4 material was around 0.7, which is similar to other result revealed by Skopp [20-21]. The friction coefficient of Si_3N_4/hBN nano/nano-composites varied from 0.30 to 0.60 and the friction coefficients of Si_3N_4/hBN micro/nano-composites were between 0.31 and 0.58. hBN has a lower friction coefficient and acts as a solid lubricant [22], hence the friction of Si_3N_4/hBN composites should decrease with the increase of hBN content. In this study, it is obvious from this figure that the friction coefficient decreased down to around 0.30 when the addition amount of hBN approaches 20 wt. %, which is much lower than the value of around 0.58 for the pure Si_3N_4 ceramics. This experimental result may be attributed to the lubrication action of hBN. Although some authors have shown that the friction coefficient is not decreased with the incorporation of hBN into Si_3N_4 [23], Kovalcikova et al. [8] reported a slight of the friction coefficient from 0.7 for Si_3N_4 to 0.64 for Si_3N_4/BN micro/nanocomposites. Also an investigation by Carrapichano et al. [24] also suggested lower friction coefficients for Si_3N_4/BN because of hBN addition at room temperature compared to that of monolithic Si_3N_4.

Figure 12 shows the variations of wear rates of friction pairs for the same experiments. From Figures 11 and 12, it could be clearly seen that, by comparison the friction and wear behaviors, the best result was obtained for the pair SN-m20/GCr15 and the pair SN-n20/GCr15. hBN contents higher than 20 % are detrimental to both wear resistance and friction properties of the ceramic composites, while the size of the Si_3N_4 starting powders (micro- or nano-sized) has a much less significant effect

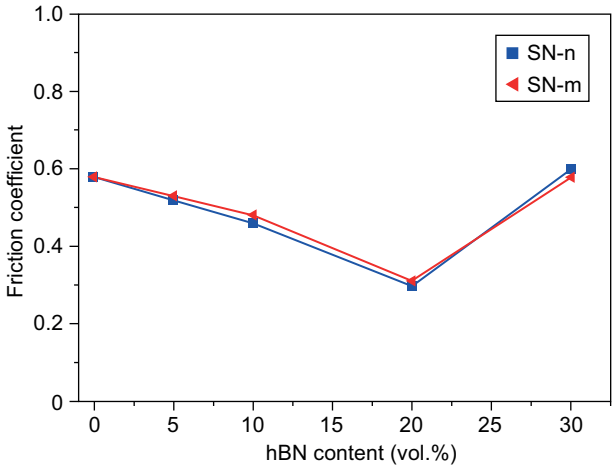

Figure 11. Effect of hBN content on the coefficient of friction of Si_3N_4/BN composites.

on the tribological characteristics of Si_3N_4 ceramic composites. Micro/nano-composites present similar friction properties and wear resistance to that of nano/nano-composites.

Figure 13 illustrates the worn surface morphologies of the SN-m20/GCr15 pair. A black film can be found on the worn surface of SN-m20 pin, as shown in Figure 13a (area "1"), and a surface film is also found on the worn surface of the GCr15 disc, as shown in Figure 13b (black area "2"). EDS results of area "1" and area "2" are shown in Figure 14. From the figures, it can be seen that the oxygen concentration in the black film of both pin and disc is observably higher, while the nitrogen concentration is much lower. It may be concluded that the black film is an oxide film, consisting of metallic and non-metallic oxides.

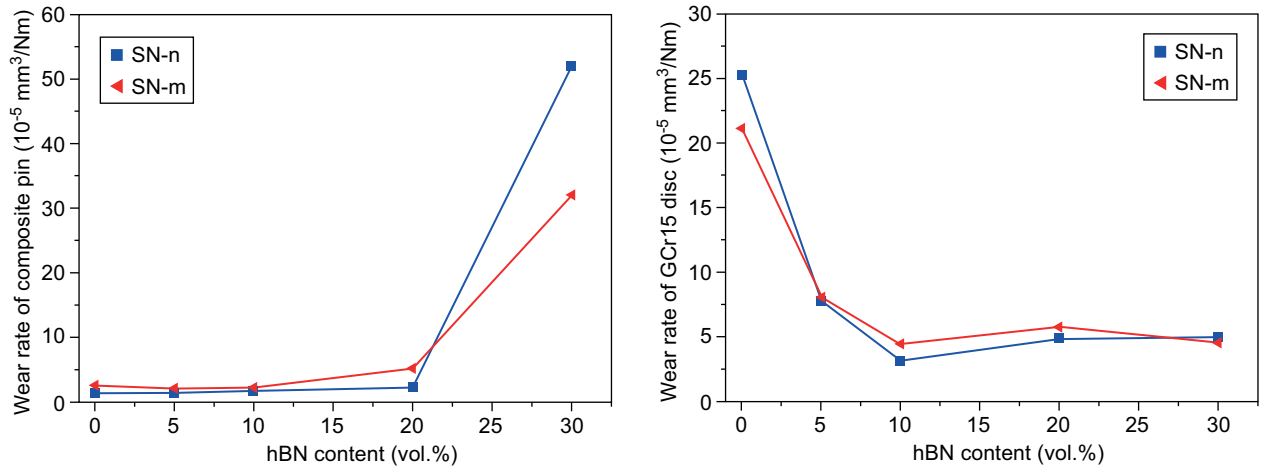

Figure 12. Effect of hBN content on the wear rates of Si_3N_4/BN/GCr15 pairs: a) pins and b) discs.

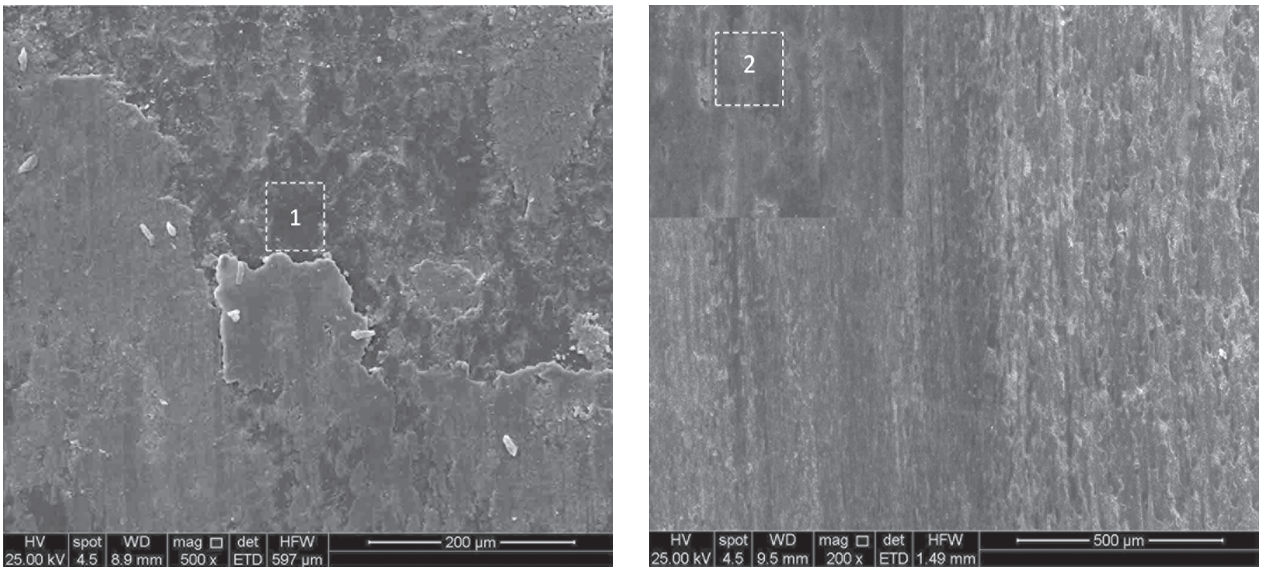

a) SN-n0 b) SN-m0

Figure 13. SEM images of SN-m20/GCr15 sliding pair: a) SN-m20 pin and b) GCr15 disc.

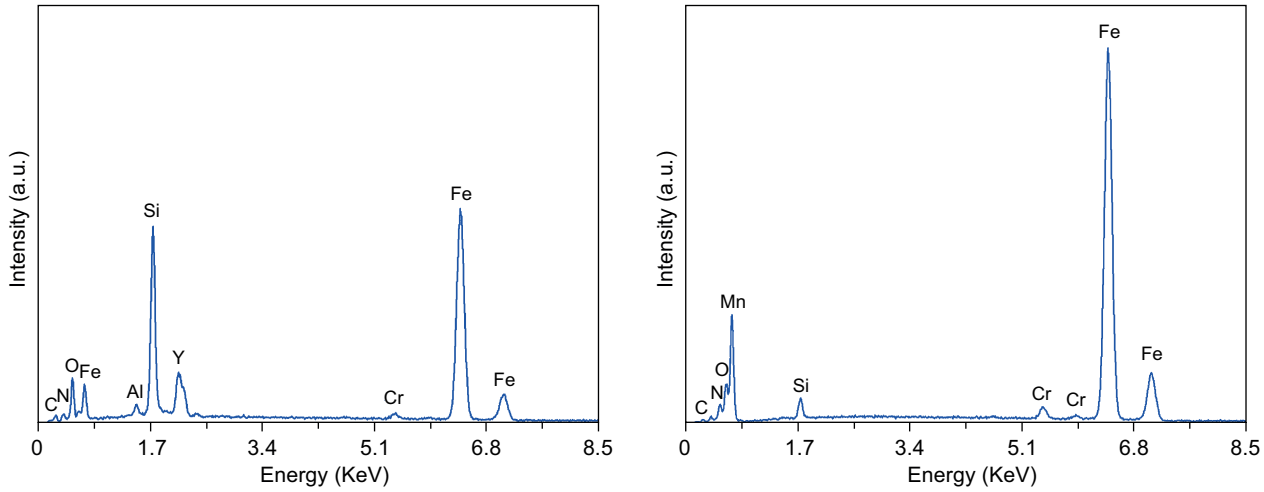

Figure 14. EDS analysis of the worn surfaces of SN-m20/GCr15 sliding pair: a) area "1" on worn surface of SN-m20 pin and b) area "2" on worn surface of GCr15 disc.

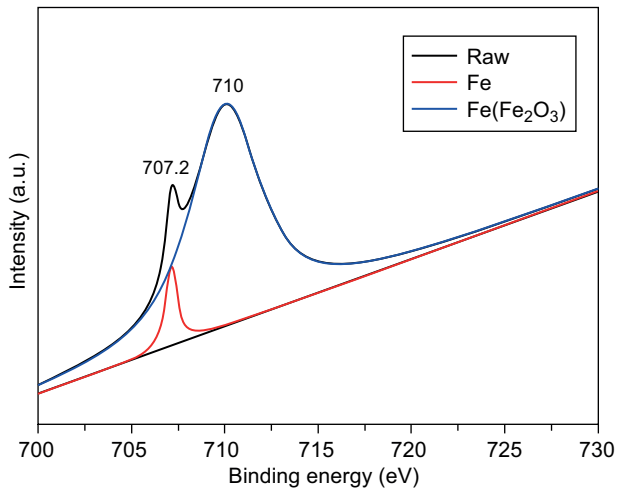

a) $Fe_{2P_{3/2}}$

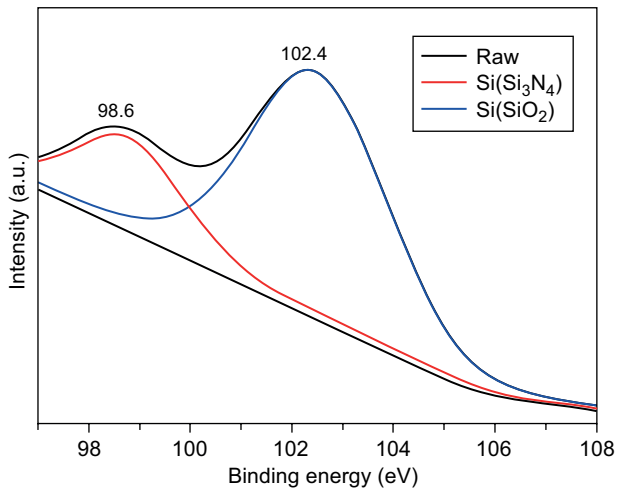

b) Si_{2p}

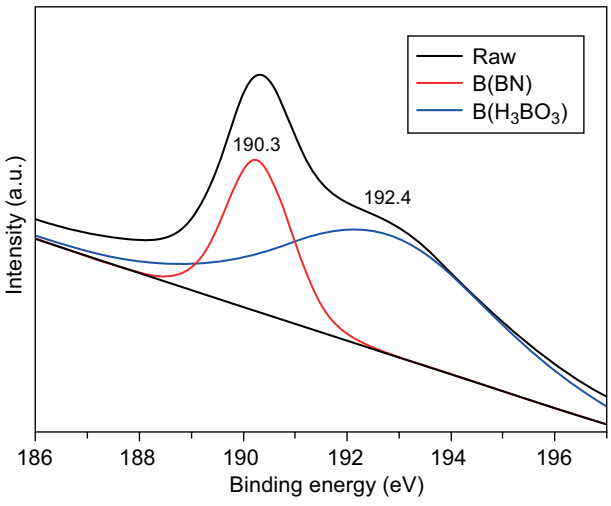

c) B_{1s}

In this study, the GCr15 disc surfaces sliding against the SN-m20 pin before and after tests were analyzed using X-ray photon spectroscopy (XPS). Through curve fitting procedure, the $Fe_{2p3/2}$, Si_{2p} and B_{1s} binding energy can be decomposed into two peaks as illustrated in Figure 15, respectively. The XPS analysis results manifest that some reaction products composed of metal oxides (Figure 15a), SiO_2 (Figure 15b) and H_3BO_3 (Figure 15c) formed on wear interface during the wear process.

Several papers [25, 26] have reported that, during sliding wear tests of ceramic/metal pairs under dry friction condition, the wear of ceramic and metal mainly results from adhesive wear or a combination of adhesive and abrasive wear. In this study, compared with austenitic stainless steel in our previous studies [13], GCr15 steel exhibits higher hardness and brittleness. When the GCr15

Figure 15. Binding energy on the worn surface of GCr15 disc sliding against SN-m20 pin under dry friction condition.

steel disc slid against the SN-m20 pin, transformed metal layers and microcracks would also continuously form on the wear surfaces of disc and pin. Some nano-scale hBN tended to detach from the micro-scale Si_3N_4 matrix, and then some smaller spalling pits formed on the pin surface. Meanwhile, a mass of wear debris would occur in the wear interface. Some wear debris accumulating in the small spalling pits reacted, leading to the formation of a tribo-chemical film (area "1" and "2" in Figure 13); the other wear debris has nowhere to accumulate, leading to abrasive wear. Therefore, the friction coefficient of SN-n20/GCr15 only reached to 0.30, which is higher than 0.03 of Si_3N_4/BN micro-composites/stainless steel. When SN-n20 pin slid against GCr15 disc, nano-scale hBN should also tend to detach from the matrix, and similar spalling pits would form on the worn surface of pin. The wear debris composed of same material to SN-m20/GCr15 pair also reacted to form a surface film. So, the friction properties and wear resistance of the SN-m20 pin slid against the GCr15 disc were almost same as that of the SN-n20 pin slid against the GCr15 disc (as shown in Figures 11 and 12).

When SN-m0 and SN-n0 pins slid against GCr15 discs, there no spalling pits are formed on the SN-m0 and SN-n0 pins, due to their higher compactness and mechanical properties. Thus, the wear debris had no chance to react with moisture in air, and no surface film formed in the wear interface. In this case, the wear mechanisms of SN-m0/GCr15 and SN-n0/GCr15 disc pairs were adhesion wear. The wear surface of GCr15 pairs sliding against SN-m0 is shown in Figure 16. SEM observation of the worn surface of GCr15 disc indicates some wear debris and the evidence of a combination of adhesion and abrasive wear. Therefore, the friction coefficient of GCr15 discs coupled with pure Si_3N_4 pins is higher than that with Si_3N_4/20 % BN pins.

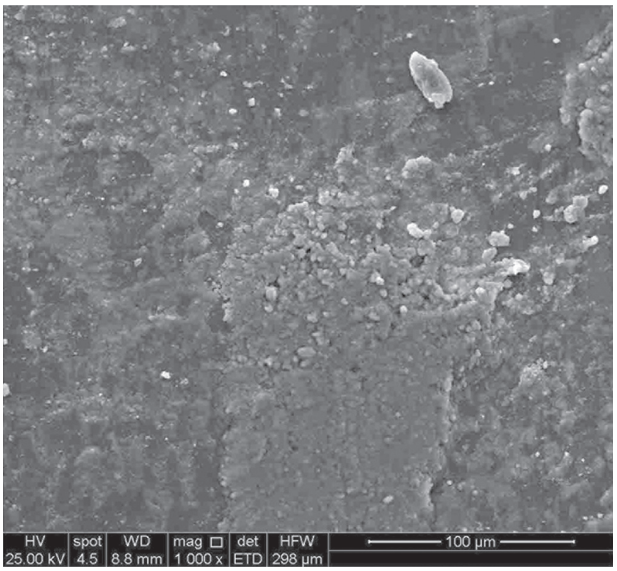

Figure 16. SEM image of GCr15 disc sliding against SN-m0 pin.

In this study, nano/micro Si_3N_4/BN composites exhibited tribological properties similar to the nano/nano Si_3N_4/BN composites due to the similar mechanical properties (as shown in Figures 6, 7 and 8). When the hBN content increased, spalling pits gradually formed on the worn surface of the ceramic composite pins. In this case, the wear debris had some space to react with moisture in air, resulting in the formation of a surface film composed of oxides. This film lubricated the wear surfaces, and lower friction coefficients and wear rates were obtained. When the hBN content is higher than 20 % (reaching up to 30 %), the poor mechanical properties would cause a large amount of wear debris and aggravate the abrasive wear, leading to a deterioration of the tribological characteristics of the Si_3N_4-30 % BN/GCr15 pair (as shown in Figures 11 and 12).

CONCLUSIONS

In the present study, nano-scale hBN was added into micro-scale and nano-scale Si_3N_4 matrix, respectively. Si_3N_4/BN ceramic composites were successfully produced via hot-pressing at 1800 °C. The effects of hBN content and the particle size of the Si_3N_4 starting powder on the physical, mechanical and tribological properties were investigated. The findings obtained in this work can be summarized as follows:

- The hBN content had a pronounced effect on the physical, mechanical and tribological performances, whereas the particle size of the Si_3N_4 starting powder did not.
- It has been shown that the bulk density, hardness, bending strength and fracture toughness of Si_3N_4/BN ceramic composites decreased with the increase of hBN content. This should be advantageous for the machinability of Si_3N_4/BN ceramic composites.
- In the wear test of Si_3N_4/20 % BN/GCr15 pairs under dry sliding condition, a tribofilm composed of metal oxides, SiO_2 and H_3BO_3 formed on the wear surfaces, resulting in a low friction coefficient and wear rate. This film lubricated the wear interface and reduced both adhesion and abrasive wear. The wear mechanism changed from a combination of adhesion and abrasive wear for the Si_3N_4/GCr15 pair to a self-lubrication mechanism for the Si_3N_4/20 % BN/GCr15 pair.

Acknowledgements

The author would like to thank Natural Science Foundation of Shaanxi Province, China (No. 2018JM5056).

REFERENCES

1. Tabandeh-Khorshid M., Omrani E., Menezes P.L., Rohatgi P.K. (2016): Tribological performance of self-lubricating aluminum matrix nanocomposites: Role grapheme nanoplatelets. *Engineering Science and Technology, 19*(1), 463-469. doi: 10.1016/j. jestch.2015.09.005
2. Zhao B., Liu H., Huang C., Wang J., Cheng M. (2017): Theoretical hardness analysis and experimental verification for composite ceramic tool materials. *Ceramic International, 43*(17), 15580-15585. doi: 10.1016/j.ceramint.2017.08.112
3. Li X., Gao Y., Wei S., Yang Q., Zhong Z. (2017): Dry sliding tribological properties of self-mated couples of B_4C-hBN ceramic composites. *Ceramic International, 43*(1), 162-166. doi: 10.1016/j.ceramint.2016.09.128
4. Zhao G., Huang C., Liu H., Zou B., Zhu H.T., Wang J. (2014): Microstructure and mechanical properties of TiB_2-SiC ceramic composites by reactive hot pressing. *International Journal of Refractory Metals and Hard Materials, 42*(1), 36-41. doi: 10.1016/j.ijrmhm.2013.10.007
5. Li X., Gao Y., Pan W., Wang X., Wu S. (2015): Fabrication and characterization of B_4C-based ceramic composites with different mass fractions of hexagonal boron nitride. *Ceramic International, 41*(1), 27-36. doi: 10.1016/j.ceramint. 2014.07.042
6. Hvizdoš P., Dusza J., Balázsi C. (2013): Tribological properties of Si_3N_4-graphene nanocomposites. *Journal of European Ceramic Society, 33*(12), 2359-2364. doi: 10.1016/j. jeurceramsoc.2013.03.035
7. Wang R., Pan W., Jiang M., Chen J., Luo Y. (2002): Investigation of the physical and mechanical properties of hot-pressed machinable Si_3N_4/h-BN composites and FGM. *Materials Science and Engineering B, 90*(3), 261-268. doi: 10.1016/S0921-5107(01)01048-0
8. Kvetková L., Duszová A., Hvizdoš P., Dusza J., Kun P., Balázsi C. (2012): Fracture toughness and toughening mecha-nisms in graphene platelet reinforced Si_3N_4 composites. *Scripta Materialia, 66*(10), 793-796. doi: 10.1016/j. scriptamat.2012.02.009
9. Kovalčíková A., Balko J., Balázsi C., Hvizdoš P., Dusza J. (2014): Influence of hBN content on mechanical and tribological properties of Si_3N_4/hBN ceramic composites. *Journal of the European Ceramic Society, 34*(14), 3319-3328. doi: 10.1016/j.jeurceramsoc.2014.02.021
10. Chen W., Gao Y.M., Wang Y., Li H. (2010): Tribological behavior of Si_3N_4-hBN ceramic materials without lubrication under different test mode. *Tribology Transactions, 53*(6), 787-798. doi: 10.1080/10402004.2010.486522
11. Chen W., Gao Y.M., Chen L., Li H. (2013): Influence of sliding speed on the tribological characteristics of Si_3N_4-hBN ceramic materials. *Tribology Transactions, 56*(6), 1035-1045. doi: 10.1080/10402004.2013.789576
12. Chen W., Gao Y.M., Ju F., Wang Y. (2009): Tribochemical behavior of Si_3N_4-hBN ceramic materials with water lubrication. *Tribology Letters, 37*(2), 229-238. doi: 10.1007/ s11249-009-9511-x
13. Chen W., Gao Y.M., Chen C. (2010): Tribological characteristics of Si_3N_4-hBN ceramic materials sliding against stainless steel without lubrication. *Wear, 269*(3-4), 241-248. doi: 10.1016/j.wear.2010.04.003
14. Chen W., Zhang D., Ai X. (2017): Effect of load on the friction and wear characteristics of Si_3N_4-hBN ceramic composites sliding against steels. *Ceramic International, 43*(5), 4379-4389. doi: 10.1016/j.ceramint.2016.12.084
15. Kusunose T., Sekino T., Chao Y.H., Niihara K. (2002): Machinability of silicon nitride/boron nitride nanocomposites. *Journal of the American ceramic society, 85*(11), 2689-2695. doi: 10.1111/j.1151-2916.2002.tb00515.x
16. Evans A.G., Charles E.A. (1976): Fracture toughness determinations by indentation. *Journal of the American Ceramic Society, 59*(7-8), 371-372. doi: 10.1111/j.1151-2916.1976. tb10991.x
17. Martin J.M., Mogne L.T., Chassagnette C. (1992): Friction of Hexagonal Boron Nitride in Various Environments. *Tribology transactions, 35*(3), 462-472. doi: 10.1080/ 10402009208982144
18. Wei D., Meng Q., Jia D. (2007): Microstructure of hot-pressed h-BN/Si_3N_4 ceramic composites with Y_2O_3-Al_2O_3 sintering additive. *Ceramic International, 33*(2), 221-226. doi: 10.1016/j. ceramint.2005.09.004
19. Cho M.W., Kim D.W., Cho W.S. (2007): Analysis of micro-machining characteristics of Si_3N_4-hBN composites. *Journal of the European Ceramic Society, 27*(2), 1259-1265. doi: 10.1016/j. jeurceramsoc.2006.08.002
20. Skopp A., Woydt M., Habig K.H. (1995): Tribological behavior of silicon nitride materials under unlubricated sliding between 22ºC and 1000ºC. *Wear, 181-183*(95), 571-580. doi: 10.1016/0043-1648(95)90173-6
21. Skopp A., Woydt M. (1992): Ceramic and ceramic composite materials with improved friction and wear properties. *Tribology Transactions, 38*(2), 233-242. doi: 10.1080/ 10402009508983400
22. Saito T., Honda F. (2000): Low friction behavior of sintered hBN sliding in sodium chloride solution. *Wear, 244*(1), 132-139. doi: 10.1016/S0043-1648(00)00451-8
23. Gutierrez-Mora F., Erdemir A., Goretta K.C., Domınguez-Rodrıguez A., Routbort J.L. (2005): Dry and oil-Lubricated sliding wear of Si_3N_4 and Si_3N_4/BN Fibrous Monoliths. *Tribology Letters, 18*(2), 231-237. doi: 10.1007/s11249-004-2747-6
24. Carrapichano J.M., Gomes J.M., Silva R.F. (2002): Tribological behavior of Si_3N_4-BN ceramic materials for dry sliding applications. *Wear, 253*(9-10), 1070-1076. doi: 10.1016/S0043-1648(02)00219-3
25. Akdogan G., Stolarski T.A. (2003): Wear in metal/silicon nitride sliding pairs. *Ceramic International, 29*(4), 435-446. doi: 10.1016/S0272-8842(02)00156-6
26. Hua M., Wei X., Li J. (2008): Friction and wear behavior of SUS 304 austenitic stainless steel against Al_2O_3 ceramic ball under relative high load. *Wear, 265*(5-6), 799-810. doi: 10.1016/j. wear.2008.01.017